



## High Performance Crystalline TiO<sub>2</sub> Mesocrystals for Enhanced Solar Fuel



A. Hegazy

National Research Centre, Solar Energy Department, El Behouth St., Dokki, Giza, Egypt.

**T**ITANIUM dioxide (TiO<sub>2</sub>) is one of the most abundant compounds in our planet. It is cheap, non-toxic, highly chemically and thermally stable semiconductor material. Titanium dioxide nanoparticles (TiO<sub>2</sub>-NPs) show high visible light transparency combined with high UV light absorption. However, altering the particle size and crystalline structure of TiO<sub>2</sub>-NPs influences the absorption range, adsorption of dye molecules and electron transfer rate at the surface. Unfortunately, TiO<sub>2</sub>-NPs suffer high electron/hole recombination rates. Therefore, an ordered superstructure consisting of nanoparticles on the scale of nanometers to several micrometers is proposed titanium dioxide mesocrystals (TiO<sub>2</sub>-MCs).

In this work, we represent a new and facile way to fabricate TiO<sub>2</sub>-MCs with spherical structure by sol-gel method. We were able to fabricate spherical TiO<sub>2</sub>-MCs with narrow size distribution by controlling the hydrolysis conditions. The effect of air annealing on the morphology, size shrinkage, and phase transition of the nanoparticles was studied by scanning electron microscopy, X-ray diffraction, and Raman spectroscopy. Also, the fabricated TiO<sub>2</sub>-MCs showed exceptional photoactivity compared to their Degussa p-25 nanoparticles counterparts upon their use in water splitting cells.

**Keywords:** TiO<sub>2</sub>, Water Splitting, Mesocrystals, Nanoparticles, Solar fuel.

### Introduction

Titanium dioxide nanoparticles (TNPs) acquired a great attention along the running decade as a cheap and efficient semi-conductor for many emerging applications such as photonic band material, gas sensing, photocatalysts and dye-sensitized solar cells (DSSCs) [1-4]. Moreover, enhanced solar energy conversion efficiency would provide enormous economic advantages [5-10].

It's known that photoactivity of (TNPs) varies greatly with its morphology [11] which can be controlled easily by varying the conditions and method of preparation. TNPs size can affect their properties such as specific surface area, life time of the exciton (e-h pair), conductivity, and surface to bulk defects [12]. Sol-gel method

has been extensively used for synthesis of TNPs due to its simple preparation technique that can be done at low temperatures as well as its low preparation cost. Due to the high reactivity of the alkoxides that are usually used as precursors for TNPs synthesis with water, HCl or KCl has been reported to reduce the reactivity of the alkoxides in addition to size control [13, 14].

Spherical TiO<sub>2</sub> NPs are of great interest to be used in solar energy conversion devices because it is required to obtain maximum photon absorption by introducing higher exposed surface area and allow infiltration of electrolyte molecules into the mesoporous TiO<sub>2</sub>. In addition, spherical particles minimize grain boundaries so that it facilitates electron transport, harvesting and minimizes recombination [1]. However, tailoring of TiO<sub>2</sub>

Corresponding author e-mail: aiathussien@gmail.com, Scopus Author ID: 56448374100

<https://orcid.org/0000-0001-6120-3467>

Received 12/6/2019; Accepted 16/6/2019

DOI: 10.21608/ejchem.2019.13610.1841

© 2019 National Information and Documentation Center (NIDOC)

NPs or design of mesoscopic TiO<sub>2</sub> structure for photoanodes have scarcely been attempted thus far, in spite of their importance in determining the performance of the photocatalytic cell [15]. Spherical particles can be synthesized from controlled hydrolysis of titanium precursors with the aid of capping agents [2]. Hydrofluoric acid has been studied widely as a capping agent for synthesis of TiO<sub>2</sub> spherical particles with an increased percentage of reactive anatase {001} facet [15] as mentioned by yang et al. [16] that {001} facet can be stabilized and produced with high percentage by F ions terminated surfaces.

With the development of new class of solid materials in order to solve the problem of charge recombination, Mesocrystals; a new class of solid materials, which can be formed through a controllable orientation of nanocrystals, have received great attention for their unique characteristics such as single crystal-like behavior, high pore volume, high crystallinity, and the perfect alignment of their subunits [17]. Having these mesocrystals is a promising alternative to single and poly crystalline materials for many applications especially in solar energy conversion and photocatalysis [18-22]. It is worth mentioning that the long-range ordered materials can significantly reduce the recombination of the e-h pairs due to the anisotropic electron flow along the interparticles [18]. A lot of work has been done for the preparation of TiO<sub>2</sub> mesocrystals [19-23]. TiO<sub>2</sub> mesocrystals was firstly reported by O'Brien's group through topotactic conversion of NH<sub>4</sub>TiOF<sub>3</sub> mesocrystals [24, 25]. Lie et al. reported a formation of TiO<sub>2</sub> mesocrystals by anisotropic dissolution of NH<sub>4</sub>TiOF<sub>3</sub> mesocrystals [26]. Also, TiO<sub>2</sub> sheets with controlled size were achieved in surfactant free aqueous solution of NH<sub>4</sub>F and TiCl<sub>4</sub> [27].

Doping of TiO<sub>2</sub> nanoparticles with transition metals like Fe, Ni, Cr and Co can greatly enhance the system efficiency such as hydrogen production via photocon version process. Amongst them cobalt won the most attention and was extensively studied as it is proved that incorporation of Co leads to a redshift in absorption hence, a decrease in energy bandgap [28, 29]. It has also been observed that cobalt-doped TiO<sub>2</sub> growth conditions are more likely to be O-poor [30, 31]. O-poor conditions lead to roughly equal concentrations of substitutional and interstitial Co, n-type behavior resulting from thermal excitation of electrons from interstitial Co into the conduction band.

Tailoring the morphology of TiO<sub>2</sub> MCs by sol-gel methods haven't been discussed widely so far. From the previous work done by Hegazy and Prouzet [32]; Hegazy et al. [33]; as well as Ahmed et al. [34], it has been concluded that the proposed synthesis way of TiO<sub>2</sub> resulted in highly ordered-template free small size of the nanoparticles with high specific surface area that enhances the efficiency of solar cells and the photocurrent density for water splitting applications. However, in this work we present a facile synthesis of TiO<sub>2</sub> MCs with submicron particles via surfactant free sol-gel method. We have followed the same recipe presented by Hegazy and Prouzet [32] except for replacing the HCl by HF. In addition, we also aim to increase the crystallinity of the mesocrystals by adding an oxidizing agent (K<sub>2</sub>S<sub>2</sub>O<sub>8</sub>) through the synthesis process. Moreover, we managed to decrease the bandgap by in situ doping the TiO<sub>2</sub> MCs with Co. The obtained results show the success of preparation of TiO<sub>2</sub> MCs with homogenous spherical shapes in the range of 1-2 μm covered by uniform plates. This synthesis resulted in bandgap narrowing and increased photocurrent density (4.2 mA/cm<sup>2</sup>), upon the use of the material in water splitting systems.

## Materials and Methods

Titanium n-propoxide (Ti(O-n-Pr)<sub>4</sub>, Aldrich) was used as the titanium source. Hydrochloric acid (HCl, 37 wt%), Formamide (FA: H<sub>2</sub>N-CHO), and Commercial P25 (Degussa P25) were purchased from Sigma-Aldrich. Potassium persulphate (K<sub>2</sub>S<sub>2</sub>O<sub>8</sub>) was used as the oxidizing agent. Hydrofluoric acid (HF 40%) was purchased from Al-Gomhoreya-Egypt. Cobalt(II) nitrate hexahydrate from Sigma-Aldrich was used as a doping agent. All the chemicals were used as received without any further purification. Fluorine-doped Tin Oxide (FTO) glass, 2.2 mm thick with a sheet resistance of 7 Ω cm<sup>-2</sup> was purchased from Solaronix.

### Preparation of titanium mesocrystals

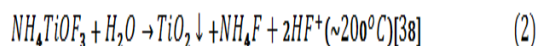
The preparation method of the TiO<sub>2</sub> mesocrystals was inspired by the proposed method detailed in Hegazy and Prouzet [31]. However, the HCl was replaced by HF. In a typical synthesis, 3ml HF was added to 5gm (Ti(O-n-Pr)<sub>4</sub> in an iced bath drop by drop. 2.4ml of DI H<sub>2</sub>O and 2.8ml formamide mixed together and added very slowly to the previous solution. The clear solution was kept at 80°C and left for aging overnight. This was the blank sample used

for comparison and was termed as HF\_RT. The sample was calcined at 400°C and termed as HF\_400. In the case of doping with Co, 0.25 gm Cobalt(II) nitrate hexahydrate was dissolved in the mixture of formamide and water and added slowly to the mixture of (Ti(O-n-Pr)<sub>4</sub> and HF and calcined at 400 (HF\_CoO\_400). This sample to enhance the crystallinity of the previous solution 0.6 gm of 0.1 M K<sub>2</sub>S<sub>2</sub>O<sub>8</sub> was added to part of the Formamide and water solution and added in the same way as the Co solution one, then annealed at 400 (HF\_CoO\_K<sub>2</sub>S<sub>2</sub>O<sub>8</sub>).

The morphological analysis of the particles was performed using a Zeiss SEM Ultra 60 field emission scanning electron microscope (FESEM). The crystal structure of the prepared samples was detected by XRD on PANalytical X'Pert PRO diffractometer. The UV-Vis absorption spectra of diluted samples in 50/50 (Ethanol:DI water) were collected using a Varian Cary 500 UV-Vis-NIR spectrophotometer, using quartz cuvette (Transparency 170–2700 nm) and 1 cm<sup>2</sup> optical path length. The Photoelectrochemical analysis was performed in 1.0 M KOH aqueous solution in a three-electrode cell configuration with Ag/AgCl electrode as reference electrode, platinum as a counter electrode and the titania sample as the working electrode using Bio-Logic SP 200 potentiostat and sunlight was simulated by 300 W Ozone-free Xenon lamp under 100 mW cm<sup>-2</sup> illumination equipped with AM 1.5 G filter.

## Results and Discussions

The TiO<sub>2</sub> mesocrystals were obtained through a facile synthesis with aid of HF. Figure 1a shows a formation of nonporous intermediate NH<sub>4</sub>TiOF<sub>3</sub> at low temperature (<200 °C). At 200 °C, the TiO<sub>2</sub> anatase appears followed the recombination reactions from precursors of Ti<sup>4+</sup>, F<sup>-</sup>, NH<sub>4</sub><sup>+</sup>, and H<sub>2</sub>O. At 400 °C NH<sub>4</sub>TiOF<sub>3</sub> is topotactically transformed into porous anatase TMCs with the dominant facets [35] as explained by the following equations (1-5) [36].



X-ray diffraction patterns show a mixture of

anatase and brookite phases as in Fig. 1b. Where peaks of 2θ = 25.3, 48.05 are assigned for {101} and {200} facets of anatase phase [40], while peaks of 2θ = 30.7, 54.7, 63.9 are assigned for {121}, {230} and {521} facets of brookite [41]. Cobalt oxide (CoO) appeared at 2θ = 36.2 and 37.4 for its {311} and {222} facets respectively [30]. Crystallite size calculated by measuring FWHM by gaussian fitting of XRD peaks and substituting in Scherrer equation:

$$L = 0. \frac{9\lambda}{A \cos\theta}$$

Where A is full width at half maximum (FWHM) in radian, L is crystallite size, λ is the wavelength of X-ray beam (0.154 nm), and θ is the incident angle for the peak center. Particle size HF\_CoO and HF\_CoO\_K<sub>2</sub>S<sub>2</sub>O<sub>8</sub> were calculated to be 7.8 nm.

From the Raman spectrum (Fig. 2), we can see clearly the characteristic E<sub>g1</sub> peak of brookite at 154 cm<sup>-1</sup> followed by E<sub>g2</sub> band at 204.17 cm<sup>-1</sup> for HF\_CoO sample while at 203.3 cm<sup>-1</sup> in HF\_CoO\_K<sub>2</sub>S<sub>2</sub>O<sub>8</sub> sample. Two B<sub>1g</sub> modes B<sub>1g1</sub>, B<sub>1g2</sub> at 393.3 cm<sup>-1</sup> and 505.5 cm<sup>-1</sup>, respectively for HF\_CoO sample, while B<sub>1g1</sub> peak is shifted to 388.13 cm<sup>-1</sup> in HF\_CoO\_K<sub>2</sub>S<sub>2</sub>O<sub>8</sub>. Finally, E<sub>g3</sub> peaks situated in 620.8 cm<sup>-1</sup> and 628.48 cm<sup>-1</sup> for HF\_CoO\_K<sub>2</sub>S<sub>2</sub>O<sub>8</sub> and HF\_CoO samples, respectively. The blue shift observed in E<sub>g1</sub> and E<sub>g2</sub> and the red shift in B<sub>1g1</sub>, B<sub>1g2</sub> and E<sub>g3</sub> modes can be explained due to crystal size going from larger to smaller sizes according to Ahmed et al. [34].

The SEM images for the undoped sample of TiO<sub>2</sub> MCs presents (Fig. 1a) both semispherical and quasi-square shape TiO<sub>2</sub> of small size ranging from 50-200 nm. Low and high-magnification SEM images of TiO<sub>2</sub>-MCs prepared with in situ doping of CoO and further treated by oxidizing agent, respectively show also both spherical and plate sheet shapes of large size between 2-3 μm. The high magnification of Fig. 3b confirms porous structure of tiny nanoparticles of size 15-20 nm.

Figure 4 depicts the UV-Vis absorption spectrum of the doped TiO<sub>2</sub> mesocrystals and further treated with potassium persulfate. It is found that there is a decrease in the bandgap to reach 2.9 eV. This bandgap narrowing can be related to the doing of Co oxide as well as the defect states that could be created by the mesocrystallinity of the particles.

Taking the bandgap narrowing and small crystalline subunit cells into consideration,

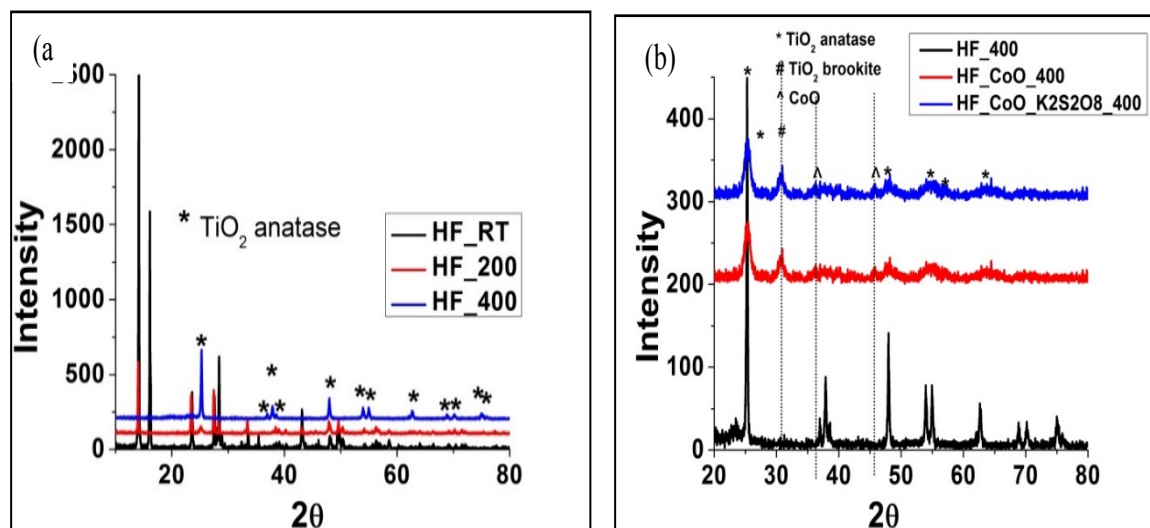


Fig. 1. XRD diffraction patterns for a) Samples prepared at RT (HF\_RT), at 200°C (HF\_200), and at 400°C (HF\_400) b) TiO<sub>2</sub> MCs in situ doped with Co (HF\_CoO) and treated with Oxidizing agent (K<sub>2</sub>S<sub>2</sub>O<sub>8</sub>) at 400°C compared to the undoped and untreated one (HF\_400).

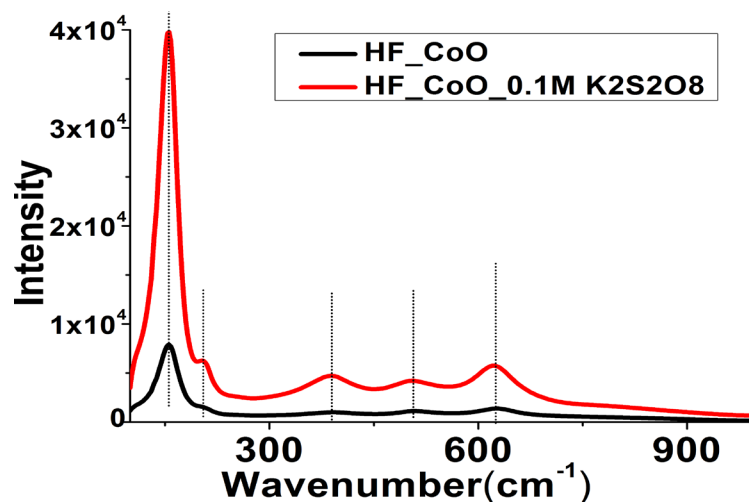


Fig. 2. Raman spectra for both TiO<sub>2</sub> MCs doped with CoO (HF\_CoO) and treated with K<sub>2</sub>S<sub>2</sub>O<sub>8</sub> (HF\_CoO\_0.1MK<sub>2</sub>S<sub>2</sub>O<sub>8</sub>).

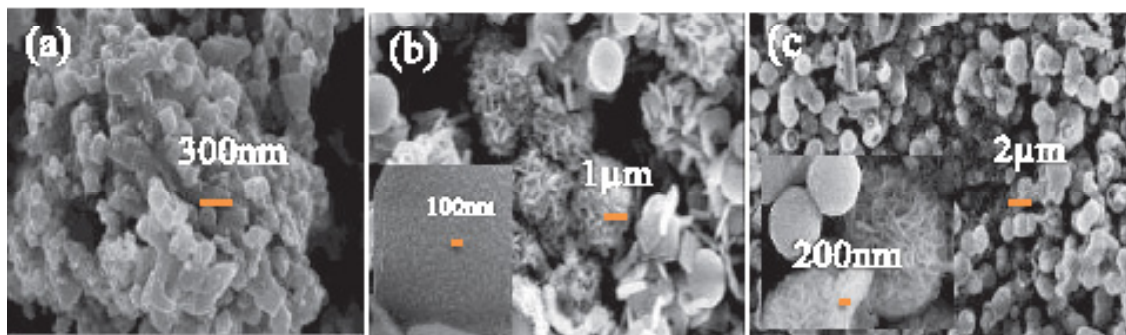


Fig. 3. FE-SEM images for (a) HF\_400 (b) HF\_CoO\_400 (inset HMSEM for the spherical particles) (c) HF\_CoO\_K<sub>2</sub>S<sub>2</sub>O<sub>8</sub>\_400 (inset is high magnification image).

we tested the mesocrystalline doped Co Oxide and treated with the oxidizing agent sample as photoanode in solar water splitting cells. Figure 5 shows higher performance toward the visible-light-driven photocatalytic water splitting, resulting in a photocurrent of 4.27 mA/cm<sup>2</sup>, which is much higher than that obtained for the commercial Degussa P25. In addition, the sample showed more negative onset potential than P25, the light contribution toward the minimum potential needed for water splitting process to take place, which can highly lead to better charge kinetics and lower consumption of applied potential.

### Conclusions

TiO<sub>2</sub> mesocrystals were successfully prepared via a facile sol gel synthesis route. The size of the mesocrystals was found to be in the range of 2-3μm with 15-20nm subunit size. This superstructure doped with Co-Oxide and further treated with oxidizing agent to enhance the sample crystallinity shows mixture phases of anatase and brookite that was induced by the doping of metals (Co). In addition, the sample exhibits a band gap narrowing of 2.9 eV and a perfect performance in photoelectrochemical water splitting application with photocurrent of 4.2eV compared to its counterpart (P25).

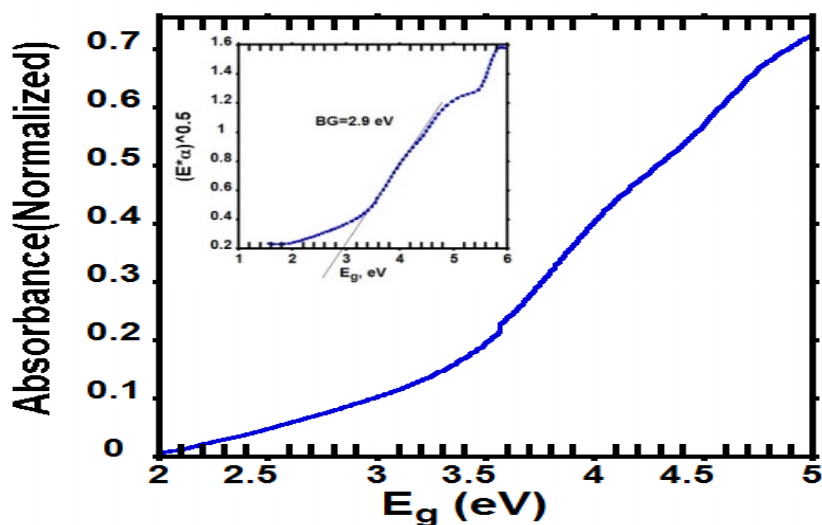


Fig. 4. Absorption spectrum of TiO<sub>2</sub>MCs(HF\_CoO\_K<sub>2</sub>S<sub>2</sub>O<sub>8</sub>) (inset is Tauc plot).

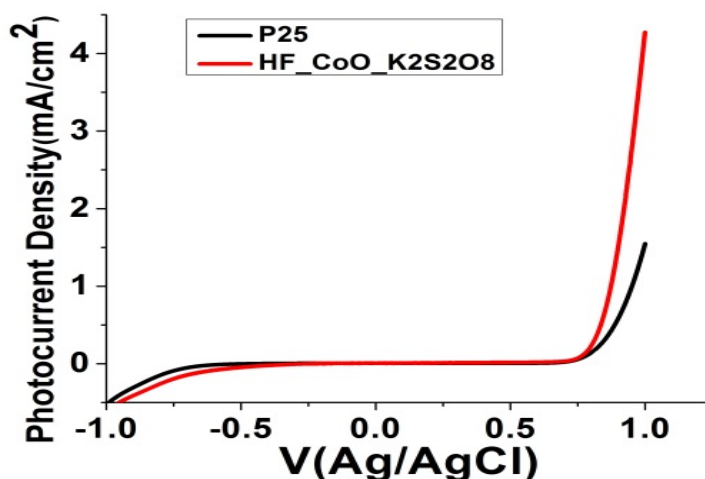


Fig. 5. The photoelectrochemical characteristics in 1M KOH aqueous solutions under AM 1.5 illumination for HF\_CoO\_K<sub>2</sub>S<sub>2</sub>O<sub>8</sub> and Degussa P25.

### Acknowledgement

National Research Centre is gratefully acknowledged for funding and supporting this work in the internal project of code: 11050113 under 11<sup>th</sup> Plane Research.

### References

- Shiba K, Sato S, Matsushita T, Ogawa M. Preparation of nanoporous titania spherical nanoparticles. *Journal of Solid State Chemistry*, **199**, 317-325 (2013).
- Lim, J.H., Um, J.H., Park, Y.J., Sung, Y.E. and Lee, J.K. Simple size control of spherical titania nanoparticles with KCl. *Bulletin of the Korean Chemical Society*, **36**(4), 1258-1261 (2015).
- Waterhouse, G.I. and Waterland, M.R. Opal and inverse opal photonic crystals: fabrication and characterization. *Polyhedron*, **26**(2), 356-368 (2007).
- Nazeeruddin MK, Gratzel M. Dye-sensitized solar cells based on mesoscopic oxide semiconductor films. *Molecular and Supramolecular Photochemistry*, **10**, 301-344 (2003).
- Chappel S, Chen SG, Zaban A. TiO<sub>2</sub>-coated nanoporous SnO<sub>2</sub> electrodes for dye-sensitized solar cells. *Langmuir*. **18**(8), 3336-3342 (2002).
- Bedja I, Kamat PV, Hua X, Lappin AG, Hotchandani S. Photosensitization of Nanocrystalline ZnO Films by Bis(2,2'-bipyridine)(2,2'-bipyridine-4,4'-dicarboxylic acid) ruthenium (II). *Langmuir*. **13**(8), 2398-2403 (1997).
- Keis K, Bauer C, Boschloo G, Hagfeldt A, Westermark K, Rensmo H, Siegbahn H. Nanostructured ZnO electrodes for dye-sensitized solar cell applications. *Journal of Photochemistry and photobiology A: Chemistry*, **148**(1-3), 57-64 (2002).
- Lewis NS, Crabtree G. Basic research needs for solar energy utilization: report of the basic energy sciences workshop on solar energy utilization, April 18-21 (2005).
- Guo P, Aegerter MA. Ru(II) sensitized Nb<sub>2</sub>O<sub>5</sub> solar cell made by the sol-gel process. *Thin Solid Films*, **351**(1-2), 290-294 (1999).
- Jiao Y, Zhang F, Meng S. Dye sensitized solar cells Principles and new design. In *Solar Cells-Dye-Sensitized Devices*, Intech Open (2011).
- Calatayud DG, Rodríguez M, Jardiel T. *Egypt. J. Chem.* **62**, Special Issue (Part 1) (2019)
- Controlling the morphology of TiO<sub>2</sub> nanocrystals with different capping agents. *Boletín de la Sociedad Española de Cerámica y Vidrio*. **54**(4), 159-165 (2015).
- N Xu, Z Shi, Y Fan, J Dong, J Shi, MZC Hu, Effects of particle size of TiO<sub>2</sub> on photocatalytic degradation of methylene blue in aqueous suspensions, *Industrial & Engineering Chemistry Research*, **38** (2), 373-379 (1999).
- Schubert, U. Chemical modification of titanium alkoxides for sol-gel processing. *Journal of Materials Chemistry*, **15**(35-36), 3701-3715(2005).
- Look, Jee L., and Charles F. Z. Alkoxide-Derived Titania Particles: Use of Electrolytes to Control Size and Agglomeration Levels. *Journal of the American Ceramic Society*, **75**(6), 1587-1595 (1992).
- Yu J, Zhang L, Huang B, Liu H. Synthesis of Spherical TiO<sub>2</sub> Made up of High Reactive Facets of. *International Journal of Electrochemical Science*, **8**, 5810-5816 (2013).
- Yang HG, Sun CH, Qiao SZ, Zou J, Liu G, Smith SC, Cheng HM, Lu GQ. Anatase TiO<sub>2</sub> single crystals with a large percentage of reactive facets. *Nature*, **453**(7195), 638-641 (2008).
- Cai, JinGuang, and LiMin Qi. TiO<sub>2</sub> mesocrystals: Synthesis, formation mechanisms and applications. *Science China Chemistry* **55**(11), 2318-2326 (2012).
- Bian, Z., Tachikawa, T., Kim, W., Choi, W. and Majima, T. Superior electron transport and photocatalytic abilities of metal-nanoparticle-loaded TiO<sub>2</sub> superstructures. *The Journal of Physical Chemistry C*, **116**(48), 25444-25453 (2012).
- Yu, X., Li, W., Huang, J., Li, Z., Liu, J. and Hu, P. Superstructure Ta<sub>2</sub>O<sub>5</sub> mesocrystals derived from (NH<sub>4</sub>)<sub>2</sub> Ta<sub>2</sub>O<sub>3</sub>F<sub>6</sub> mesocrystals with efficient photocatalytic activity. *Dalton Transactions* (2018).
- Zhu, G., Solits, J., Tao, J., Legg, B., Wang, C. and de Yoreo, J. Alternate Path to the Formation of Co-aligned Hierarchical Mesocrystals, In *APS Meeting Abstracts* (2018).
- Tan, B., Zhang, X., Li, Y., Chen, H., Ye, X., Wang, Y., & Ye, J. Back Cover: Anatase TiO<sub>2</sub> Mesocrystals: Green Synthesis, In Situ Conversion to Porous Single Crystals, and Self-Doping Ti<sup>3+</sup>

- for Enhanced Visible Light Driven Photocatalytic Removal of NO. *Chemistry—A European Journal*, **23**(23), 5626-5626 (2017).
22. Hong, Z., Zhou, K., Zhang, J., Huang, Z., & Wei, M. Facile synthesis of rutile TiO<sub>2</sub> mesocrystals with enhanced sodium storage properties. *Journal of Materials Chemistry A*, **3**(33), 17412-17416 (2015).
23. Zhou L, Smyth-Boyle D, O'Brien P. Uniform NH<sub>4</sub>TiOF<sub>3</sub> mesocrystals prepared by an ambient temperature self-assembly process and their topotaxial conversion to anatase. *Chemical Communication*, 144–146 (2007).
24. Zhou L, Smyth-Boyle D, O'Brien P. A facile synthesis of uniform NH<sub>4</sub>TiOF<sub>3</sub> mesocrystals and their conversion to TiO<sub>2</sub> mesocrystals. *Journal of American Chemical Society*, **130**, 1309–1320 (2008).
25. Liu YQ, Zhang Y, Tan H, Wang J. Formation and anisotropic dissolution behavior of NH<sub>4</sub>TiOF<sub>3</sub> mesocrystals. *Crystal Growth & Design*, **11**, 2905–2912 (2011).
26. Feng J, Yin M, Wang Z, Yan S, Wan L, Li Z, Zou Z. Facile synthesis of anatase TiO<sub>2</sub> mesocrystal sheets with dominant {001} facets based on topochemical conversion. *Cryst. Eng. Comm.*, **12**(11), 3425–3429 (2010).
27. Song, R.Q. and Cölfen, H. Mesocrystals—Ordered nanoparticle superstructures. *Advanced Materials* **22**(12), 1301-1330 (2010).
28. Khan MA, and Yang OB. Photocatalytic water splitting for hydrogen production under visible light on Ir and Co ionized titania nanotube. *Catalysis Today*, **146**(1-2), 177-82 (2009).
29. Stella C, Prabhakar D, Soundararajan N, and Ramachandran K. Effect of cobalt doping on structural, optical and dielectric properties of TiO<sub>2</sub>. *In AIP Conference Proceedings 2016 May 23* (Vol. 1731, No. 1, p. 050020). AIP Publishing.
30. Matsumoto, Y., Murakami, M., Shono, T., Hasegawa, T., Fukumura, T., Kawasaki, M. & Koinuma, H. Room-temperature ferromagnetism in transparent transition metal-doped titanium dioxide. *Science*, **291**(5505), 854-856 (2001).
31. Chambers SA, Thevuthasan S, Farrow RF, Marks RF, Thiele JU, Folks L, Samant MG, Kellock AJ, Ruzycski N, Ederer DL, Diebold U. Epitaxial growth and properties of ferromagnetic co-doped TiO<sub>2</sub> anatase. *Applied Physics Letters*, **79**(21), 3467-9346 (2001).
32. Aiat H., Eric P. Room Temperature Synthesis and Thermal Evolution of Porous Nanocrystalline TiO<sub>2</sub> Anatase, *Chemistry of Materials*, **24**, 245-254 (2012).
33. Hegazy, A., Kinadjian, N., Sadeghimakki, B., Sivoththaman, S., Allam, N. K., & Prouzet, E. TiO<sub>2</sub> nanoparticles optimized for photoanodes tested in large area Dye-sensitized solar cells (DSSC). *Solar Energy Materials and Solar Cells*, **153**, 108-116 (2016).
34. Ahmed El-Sayed, Nada Atef, Aiat H. Hegazy, K.R. Mahmoud, R.M. Abdel Hameed, Nageh K. Allam. Defect states determined the performance of dopant-free anatase nanocrystals in solar fuel cells. *Solar Energy*, **144**, 445–452 (2017).
35. Fujishima, A., Xintong Z., and Donald A. Tryk. TiO<sub>2</sub> photocatalysis and related surface phenomena. *Surface Science Reports* **63**(12), 515-582 (2008).
36. Zhang, Peng, Mamoru F., and Tetsuro M. Development of tailored TiO<sub>2</sub> mesocrystals for solar driven photocatalysis. *Journal of Energy Chemistry* **25**(6), 917-926 (2016).
37. Bian, Zhen F., Takashi T., and Tetsuro M. "Superstructure of TiO<sub>2</sub> crystalline nanoparticles yields effective conduction pathways for photogenerated charges." *The Journal of Physical Chemistry Letters* **3**(11), 1422-1427 (2012).
38. Zhou, L., Smyth-Boyle, D. and O'Brien, P. A facile synthesis of uniform NH<sub>4</sub>TiOF<sub>3</sub> mesocrystals and their conversion to TiO<sub>2</sub> mesocrystals. *Journal of the American Chemical Society*, **130**(4), 1309-1320 (2008).
39. Lee, H.K. and Lee, S.W. Surfactant-free NH<sub>4</sub>TiOF<sub>3</sub> crystals: self-assembly on solid surfaces and room-temperature hydrolysis for hollow TiO<sub>2</sub> structures with high photocatalytic activity. *Chemistry Letters*, **44**(5), 604-606 (2015).
40. Di Paola, A., Bellardita, M. and Palmisano, L. Brookite, the least known TiO<sub>2</sub> photocatalyst. *Catalysts*, **3**(1), 36-73 (2013).
41. Yang J, Liu H, Martens WN, Frost RL. Synthesis and characterization of cobalt hydroxide, cobalt oxyhydroxide, and cobalt oxide nanodiscs. *The Journal of Physical Chemistry C*, **114**(1), 111-9 (2009).

## الاداء الامثل لبلورات اكسيد التيتانيوم المتناهية الصغر لانتاج الوقود الشمسي

ايات حجازي

قسم الطاقة الشمسي - المركز القومي للبحوث - الجيزة - مصر.

ثاني اكسيد التيتانيوم هو واحد من اكثر المركبات وفرة في كوكبنا. و يعتبر ثاني اكسيد التيتانيوم مادة شبة موصلة حيث يتميز بانه رخيص، غير سام، مستقر كيميائيا وحراريا. نتيجة لهذه المميزات فقد تم استخدام اكسي التيتانيوم بكثرة كقطب ضوئي لانتاج الهيدروجين بطريقة كهروكيميائية في وجود ضوء الشمس المباشر. و تعتبر هذه الطريقة هي الاكثر شيوعا في انتاج الهيدروجين و الذي يعتبر وقود غير تقليدي حيث يعتمد انتاجه علي وجود مصدر طاقة متجدد (الشمس). تظهر جسيمات ثاني اكسيد التيتانيوم النانومترية شفافية عالية للضوء المرئي الي جانب امتصاص ضوئي عالي للاشعة فوق البنفسجية. و مع ذلك فان تغيير حجم الجسيمات و البنية البلورية لجزيئاته تؤثر علي نطاق الامتصاص و معدل نقل الالكترتون علي السطح. لسوء الحظ فان بلورات اكسيد التيتانيوم النانومترية تعاني من ارتفاع معدل الربط بين الالكترتون و الفجوة. و تمت معالجة هذه المشكلة بتحضير بلورات اكسيد التيتانيوم بطريقة تجعل البلورات المكونة من جسيمات متناهية الصغر بمقياس النانومتر تترتب بشكل منتظم لدرجة عالية. في هذا البحث تم تحضير جزيئات اكسيد التيتانيوم الكروية بطريقة سهلة و مبتكرة بتوزيع ضيق للحجم من خلال التحكم في ظروف التحلل المائي خلال التحضير بطريقة المحلول الغرواني حيث يتم تطوير المحلول تدريجيا لتكوين نظام ثنائي الطور يشبه الهلام يحتوي علي كل من الطور السائل و المواد الصلبة التي تتراوح اشكالها من الجزيئات المنفصلة الي شبكات البوليمرات المستمرة. تمت دراسة تالدين الهواء علي التشكل، و انكماش الحجم، وانتقال الطور في الجسيمات النانومترية عن طريق المجهر الالكتروني، و حيود الاشعة السينية، و طيف رامان. كما اظهرت هذه البلورات نشاطا ضوئيا استثنائيا مقارنة مع نظرائهم التجارية " ديجوسا ٢٥" عند استخدامها في انتاج الوقود الشمسي.